Journal of Applied Polymer Science

$LaF_3 : Eu^{3+}$ Nanocrystal/PNIPAM Nanogels: Preparation, Thermosensitive Fluorescence Performance and Use as Bioprobes for Monitoring Drug Release

Yang Yang, Qiusheng Song, Kang Gao, Haihong Ma, Sensen Yang, Tan Li
School of Chemical Engineering, Hefei University of Technology, Hefei 230009, China
Correspondence to: Q. Song (E-mail: sqshfut@126.com)

ABSTRACT: Novel core–shell $LaF_3 : Eu^{3+}$ nanocrystals/PNIPAM nanogels were prepared by surface-initiated living radical polymerization. The microstructure and performance of the $LaF_3 : Eu^{3+}$ nanocrystals and the hybrid nanogels were characterized by transmission electron microscopy (TEM), X-ray diffraction (XRD), X-ray photoelectron spectrometer (XPS), and photoluminescence (PL). The thermosensitive fluorescence behaviors of the core–shell nanogels and the drug release behaviors were investigated by PL at various temperatures. The results suggested that the fluorescence performance of the nanogels was influenced greatly by the ambient temperature, either content of Aspirin absorbed in the nanogels. Compared to other reported systems, our discovery could tell how much the nanogels contain Aspirin by detecting the fluorescence intensity. © 2013 Wiley Periodicals, Inc. J. Appl. Polym. Sci. **2014**, *131*, 39930.

KEYWORDS: microgels; drug delivery systems; phase behavior

Received 15 May 2013; accepted 4 September 2013
DOI: 10.1002/app.39930

INTRODUCTION

Core–shell nanogels are a new series of functional nanomaterials, because they combine different chemical composition either in the core or shell. Up till now, many core–shell nanogels have been fabricated by different synthetic strategies, and their unique performance is attractive for application in catalysis, photonics, electronics, optics, biomedicine, and so on.[1,2] Amongst them, environmentally stimuli-responsive core–shell nanogels are the most investigated ones.[3–6]

As well be known, PNIPAM gels can undergo a reversible phase transition at about 32°C. It means that below the lower critical solution temperature (LCST) the nanogels are swollen and above the LCST they are collapsed.[7,8] This unique performance makes PNIPAM based nanogels to be an important nanomaterial for controlled drug release. For example, Duan et al.[9] synthesized chitosan-*grafted*-poly(*N*-isopropylacrylamide) (CS-*g*-PNIPAm) nanogels displaying well released behaviors. Li et al.[10] prepared a novel temperature and UV dual-responsive poly(*N*-isopropylacrylamide(PNIPAM)-*co*-Chlorophyllin) nanogel via the surfactant-free emulsion polymerization. The novel dual functional nanogel is potent for improving the drug-release profile. Yallapu et al.[11] synthesized poly(*N*-isopropylacrylamide) (PNIPAM) nanogels using free-radical cross-linking polymerization, and the nanogels can be used for intravascular delivery of rapamycin.

On the other hand, rare-earth nanocrystals are another family of important nanomaterials due to their unique optical and electronic properties.[12–17] For example, due to their 4*f*-intraconfigurational transitions are independent of crystalline size and shape, therefore, it is unnecessary to strictly control the size monodispersity in synthesis to reach spectral purity. Furthermore, multicolor emissions of rare-earth nanocrystals can be achieved easily by doping different lanthanide ions for their abundant electron transitions. Moreover, rare-earth nanocrystals are well distinguishable from other chromophores in signal output because of their long luminescent lifetimes; this benefits time-gated detection techniques through enhanced signal-to-noise ratios. Therefore, rare-earth nanocrystals are potential bioprobes, and they may play an important role in many application areas, such as, optics, optoelectronics, biological labeling, and catalysis fields.[18–22]

Hence, incorporation of rare-earth nanocrystals with PNIPAM nanogels provides an attracted area.[23–25] Recently, our group has reported a series of nanocrystals/PNIPAM complex hydrogels.[24–26] These complex hydrogels have presented unique thermosensitive fluorescence performance, and that makes these complex hydrogels suitable to be used as sensors and actuators.[27] In our opinion, these complex gels may be promising materials for monitoring drug release. Because they can not only carry out the controlled drug release, but also the drug-

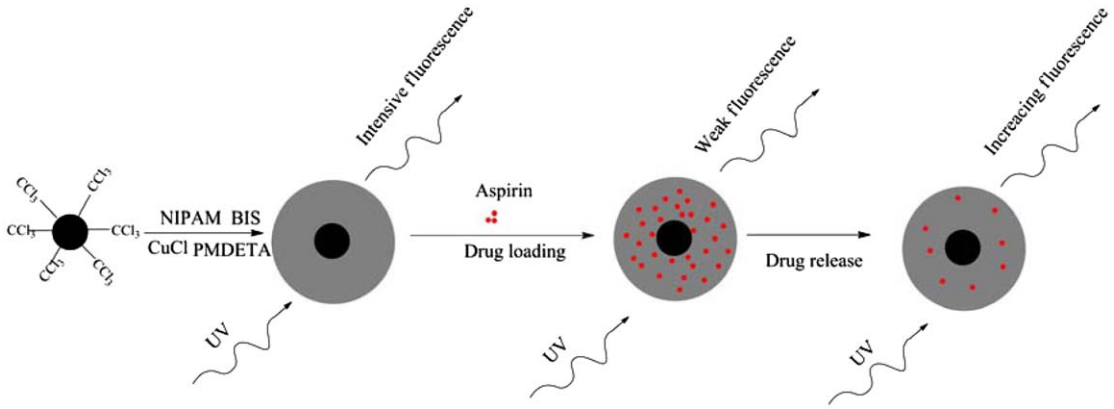

Scheme 1. Schematic illustration of synthesis of LaF_3 : Eu^{3+}/PNIPAM core–shell nanogel and its traced drug loading and release behavior. [Color figure can be viewed in the online issue, which is available at wileyonlinelibrary.com.]

loading and release behaviors can be easily traced by PL. Unfortunately, till now, few reports can be available on the drug-loading and release behaviors and mechanism about rare-earth nanocrystals based nanogels.

Herein, we report a novel core–shell nanogel which involves LaF_3 : Eu^{3+} nanocrystals as core, and thermosensitive PNIPAM as outer shell. As presented in Scheme 1, such well-designed core–shell hybrid nanogels are promising to load and release of target drug. Aspirin was used as a model drug to assess the loading and controlled releasing behaviors of this novel kind of core–shell hybrid nanogels. The LaF_3 : Eu^{3+} nanocrystals emit special photoluminescence, and the LaF_3 : Eu^{3+} nanocrystals/PNIPAM core–shell nanogels present unique thermosensitive fluorescence performances. The fluorescence intensity of the nanogels decreases gradually with the increase of Aspirin content. Compared to other reported systems, our discovery could tell how much the hybrid nanogels contain Aspirin by detecting the fluorescence intensity.

EXPERIMENTAL

Materials

Europium nitrate hexahydrate ($Eu(NO_3)_3{\cdot}6H_2O$) and lanthanum nitrate hexahydrate ($La(NO_3)_3{\cdot}6H_2O$, purity >99.9%) were purchased from the Shanghai Chemical Reagent Company Co., China and used as received without further purification. Pentamethyldiethylenetriamine (PMDETA), carbon tetrachloride (CCl_4), sodium fluoride, undecylenic acid, sodium oleate, sodium hydroxide, ethanol, chloroform, tetrahydrofuran (THF), and *N,N′*-methylenebisacrylamide (BIS) were of reagent grade quality and purchased from Beijing Chemical Reagent Company Co., China and used as received without further purification. *N*-Isopropylacrylamide (NIPAM) was recrystallized in hexane. Benzoyl peroxide (BPO) was recrystallized in methanol. Cuprous chloride (CuCl) was soaked into acetic acid, filtered and washed with acetone before used. Aspirin was purchased from Beijing Shuangqiao Pharmaceutical Company. Water was deionized and obtained from an Elga Option 4 system.

Preparation of LaF_3: Eu^{3+} Nanocrystals

First, the reactants of sodium oleate (1.2 g), H_2O (20 mL), ethanol (10 mL), undecylenic acid (5 mL), NaF (0.224 g), $Eu(NO_3)_3{\cdot}6H_2O$ (0.08 g), and $La(NO_3)_3{\cdot}6H_2O$ (0.7 g) were put into a Teflon bottle held in a stainless steel autoclave with the volume of 50 mL. Then the autoclave was sealed and maintained at 120°C for 10 h. After that, the autoclave was cooled to room temperature, and the upper liquid was discarded. The precipitate was then centrifuged and washed with ethanol to remove possible remnants in the final products. After the operation was repeated three times; the LaF_3 : Eu^{3+} nanocrystals were finally centrifuged and dried at 80°C in air.

Synthesis of LaF_3: Eu^{3+} Nanocrystals Decorated with $-CCl_3$ Groups on Their Surface

The as-prepared LaF_3 : Eu^{3+} nanocrystals (0.3 g) and CCl_4 (8 mL) were added into a 10 mL sealing tube, and the tube was placed into ultrasonic oscillator about 30 min. After the addition of BPO (0.288 g), the tube was put into an ice bath and vacuum was exerted on it for 5 min. After that, the tube was sealed and kept at 75°C for 5 h; meanwhile the mixture was stirred with a magnetic stirrer. The product was then centrifuged and washed with ethanol to remove possible remnants in the final products. After the operation was repeated three times; the $NaYF_4$: Eu^{3+} nanocrystals decorated with $-CCl_3$ groups on their surface were obtained by drying at 60°C under vacuum.

Preparation of Core–Shell LaF_3: Eu^{3+}/PNIPAM Nanogels

In a typical synthesis, 0.05 g the as-prepared functional LaF_3 : Eu^{3+} nanocrystals, 2-propanol (4 mL), and the reactants of NIPAm/BIS/PMDETA/CuCl (mole ratio 180 : 1 : 1 : 1; $n_{NaYF4:Eu3+}/n_{NIPAm} = 1/500$) were mixed and added into a 10 mL sealing tube. The tube was placed into an ultrasonic oscillator about 10 min to obtain a uniform mixture, and then the tube was put into an ice bath and the oxygen was removed by exerting vacuum on the tube for about 5 min. After the operation was repeated three times, the tube was sealed and kept stirring at room temperature for 2 h. After that, the crude nanogels were synthesized. Finally, the crude nanogels were immersed into deionized water to remove the remained monomers and impurities, then were centrifuged at speed 14,000 rpm and washed with water three times. The nanogels were obtained by vacuum drying at 50°C.

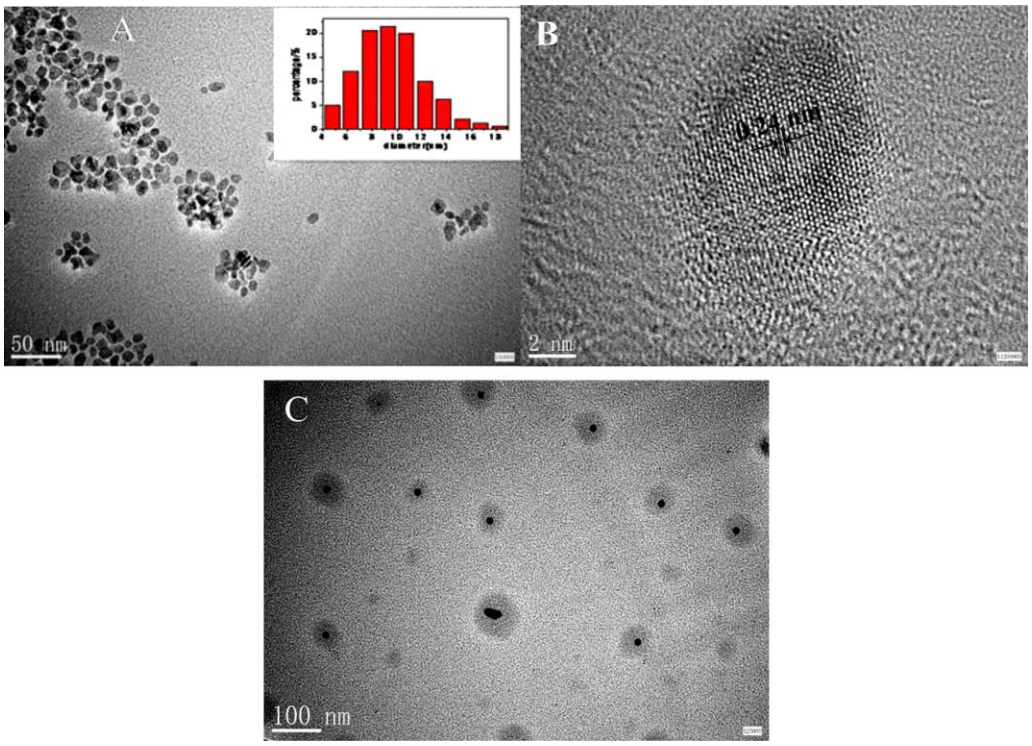

Figure 1. HRTEM images of LaF_3 : Eu^{3+} nanocrystals and the nanogels. [Color figure can be viewed in the online issue, which is available at wileyonlinelibrary.com.]

In Vitro Aspirin Loading and Release

The core–shell LaF_3 : Eu^{3+}/PNIPAM nanogels (6 mg) were dispersed in 2 mL of deionized water, and 2 mL of Aspirin (10 mg/mL) was added into the above solution. The mixture was shaken for 24 h at room temperature to reach the equilibrium state. Then the solution was centrifuged to collect the Aspirin-loaded nanogels. Each supernatant solution was collected, and the content of Aspirin was determined by UV–vis spectral measurement at the wavelength of 297 nm. After that, Aspirin-loaded nanogels were immersed in 2 mL of phosphate buffered saline (PBS) (pH =7.4) solution at 37°C. At selected time intervals, buffer solution was taken and replaced with fresh buffer solution. The amounts of released Aspirin in the supernatant solutions were measured by a UV–vis spectrophotometer. The fluorescence spectra of the nanogels were analyzed with fluorescence spectrometer at excited wavelength 300 nm.

Characterization

The morphologies and the structures of the as-synthesized samples were characterized using X-ray diffraction (XRD, Rigaku D/Max-rB with Cu $K\alpha$ radiation) and transmission electron microscopy (TEM, JEM-2100F). The fluorescence performance was investigated with a Hitachi F-4600 fluorescence spectrophotometer with a temperature range of 25–50°C. XPS spectrum was recorded on a Thermo ESCALAB 250 X-ray photoelectron spectrometer with a monochromatic Al $K\alpha$ as X-ray source. The Ultraviolet–visible spectrum of Aspirin was recorded on an Ultraviolet spectrophotometer (UV–vis, Shimadzu UV-2550).

RESULTS AND DISCUSSION

Microstructure

The morphology of the LaF_3 : Eu^{3+} nanocrystals was examined by means of TEM. Figure 1 shows the TEM images of LaF_3 : Eu^{3+} nanocrystals. The images reveal that the LaF_3 : Eu^{3+} nanocrystals have good monodispersity. And the size of which is about 4–19 nm calculated via NanoMeasure1.2 software (Figure 1 inset). Their main size of which is 7–11 nm and the space of the plane is 0.24 nm [Figure 1(B)].

The image [Figure 1(C)] confirms that the nanogels are core–shell nanoparticles, and their size is about 50–100 nm.

In order to investigate the crystal phase of the nanocrystals, XRD was performed and the XRD pattern is presented in Figure 2, which indicates that all labeled diffraction peaks at 27.7°, 43.8°, 44.8°, 50.6°, and 52.7° correspond to the crystal planes (111), (330), (113), (220), and (221). And, these facts confirm the existence of hexagonal LaF_3 : Eu^{3+} (JCPDS card 32–0483) in the nanocrystals.[22,28]

To further confirm the chemical composition of the nanogels, XPS spectra were recorded in Figure 3. According to the spectrum shown in Figure 3(A) for the nanocrystals, the binding energy for La3d^5, F1s, and Eu4d are observed at 836, 684, and 135 eV, respectively. The peak at 284 eV for C1s is ascribed to C–H groups, and the peak of O1s at 531 eV is attributed to C=O bonding. These signals reveal that the surface of the nanocrystals has been covered with undecylenic acid molecules.

As for the functional nanocrystals [Figure 3(B)], besides the above all characteristic peaks observed in the nanocrystals, new

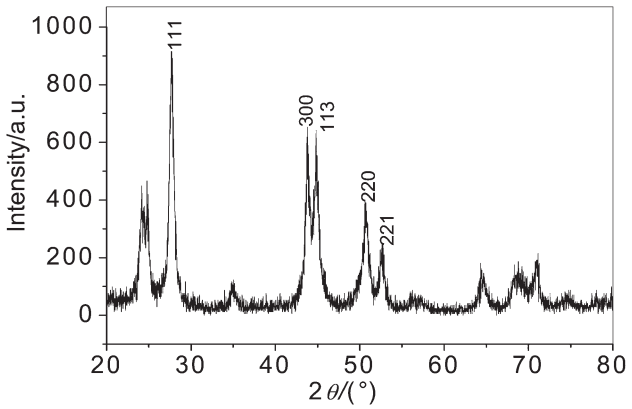

Figure 2. XRD pattern of LaF_3 : Eu^{3+} nanocrystals.

peak of Cl2p at 197 eV which arises from –C–Cl is checked, implying that the nanocrystals have been activated by BPO and CCl_4, and C–Cl groups have been introduced onto the surface of the nanocrystals.

As the results shown in Figure 3(C) of the nanogels, besides of the peaks of C1*s* and O1*s*, a new peak of N1*s* is found at 397 eV. It may be resulted from the N in the network of PNIPAM. Due to no any N element in the surface of nanocrystals, this signal further confirms that the core–shell nanogels have been fabricated.

PL Performance

To investigate the PL performance of the LaF_3 : Eu^{3+} nanocrystals, the PL spectrum was recorded in Figure 4. In the spectrum shown in Figure 4, under exciting wave of 300 nm, two characteristic emission peaks at 592 and 615 nm are observed, which are ascribed to LaF_3 : Eu^{3+} nanocrystals. Among them, the peak at 592 nm is resulted from the $^5D_0 \rightarrow {}^7F_1$ transition, and peak at 615 nm is ascribed to the $^5D_0 \rightarrow {}^7F_2$ transition of Eu^{3+}.[18,19]

In order to further investigate the thermosensitivity performance, PL spectra of the nanogels at different temperatures were also recorded, and the PL spectra are shown in Figure 5.

The results indicate that emission peaks of the nanogels are centered on 593 and 616 nm, which demonstrates that the emission peaks of the nanogels are in accordance with those of the nanocrystals.

The intensity enhanced abruptly with the increasing temperature and the higher the ambient temperature, the greater the intensity. These results suggest that the fluorescence intensity of the nanogels is significantly correlated with the ambient temperature, and the results of PL spectra demonstrate that the variations of the fluorescence intensity of the nanogels are well consistent with their phase transition. That is, the volume of the nanogels varied sharply with the variation of ambient temperature. Meanwhile, the fluorescence intensity of nanogels changed abruptly. Generally speaking, PNIPAM hydrogel does

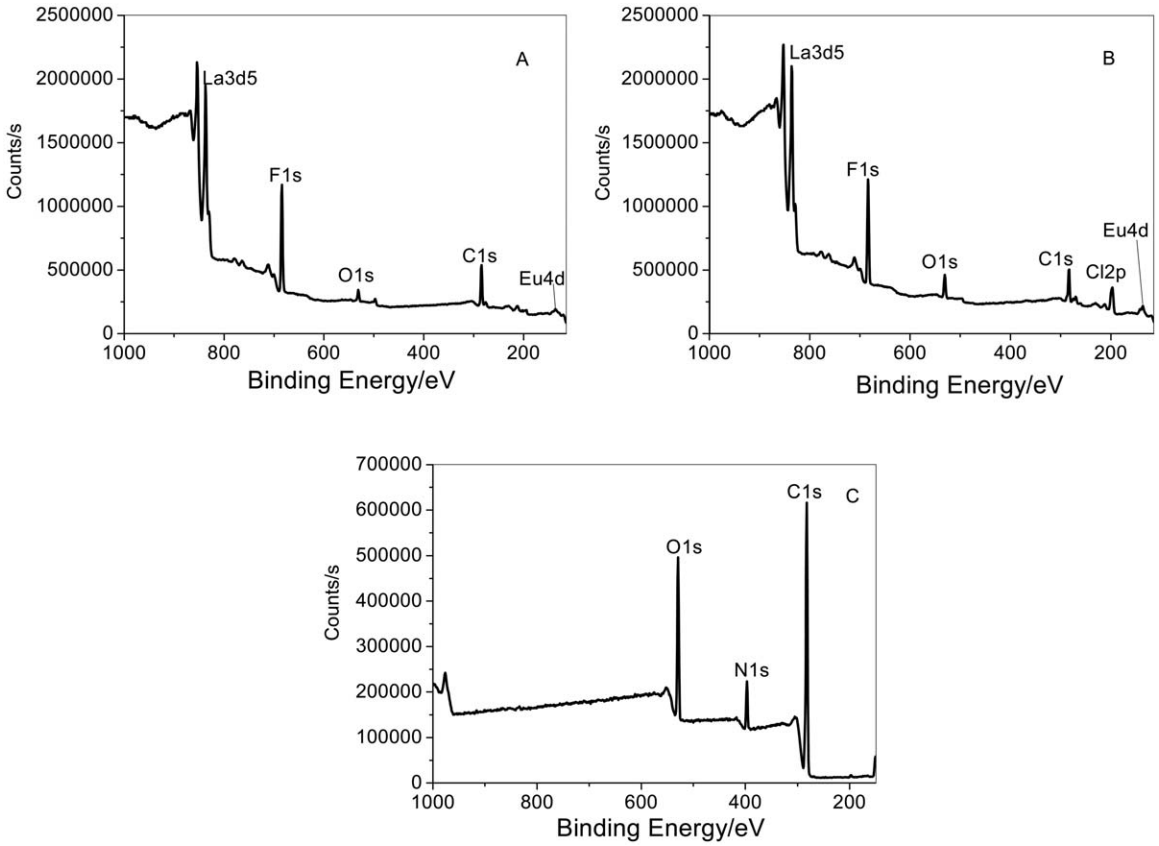

Figure 3. XPS spectra of the as-prepared samples: (A) nanocrystals, (B) functional nanocrystals, and (C) core–shell nanogels.

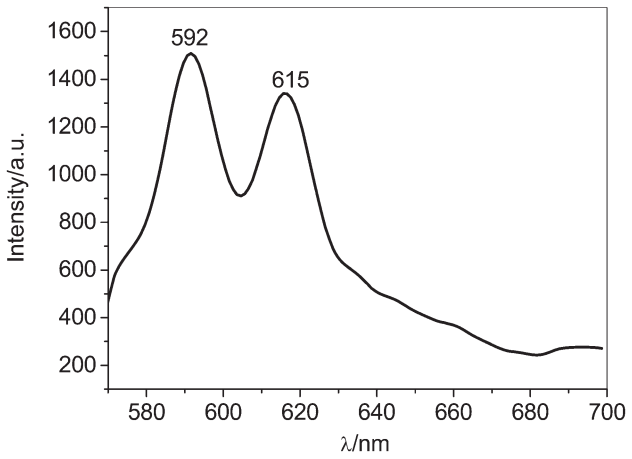

Figure 4. PL spectrum of $LaF_3 : Eu^{3+}$ nanocrystals ($\lambda ex = 300$ nm).

not emit fluorescence; therefore, the fluorescence emission of the nanogels is derived from the nanocrystals.

In order to further discuss the thermosensitive fluorescence behavior of nanogels, the intensity of the peak, which raises around 593 nm of the nanogels at different ambient temperatures and different concentrations in Figure 5, is plotted in Figure 6. The results of Figure 6 indicate that the concentration of the nanogels in water is another factor to influence their fluorescence performance. For example, when the concentration of the nanogel is kept at 10%, the ambient temperature induced thermosensitive fluorescence behavior is different from other tested samples, which may be resulted from its lower concentration (≤10%). In the other aspect, with the increasing concentration of the nanogels in water, all other samples present sharply transition around their LCST. And when the concentration is raised as higher as 60%, the fluorescence intensity of the

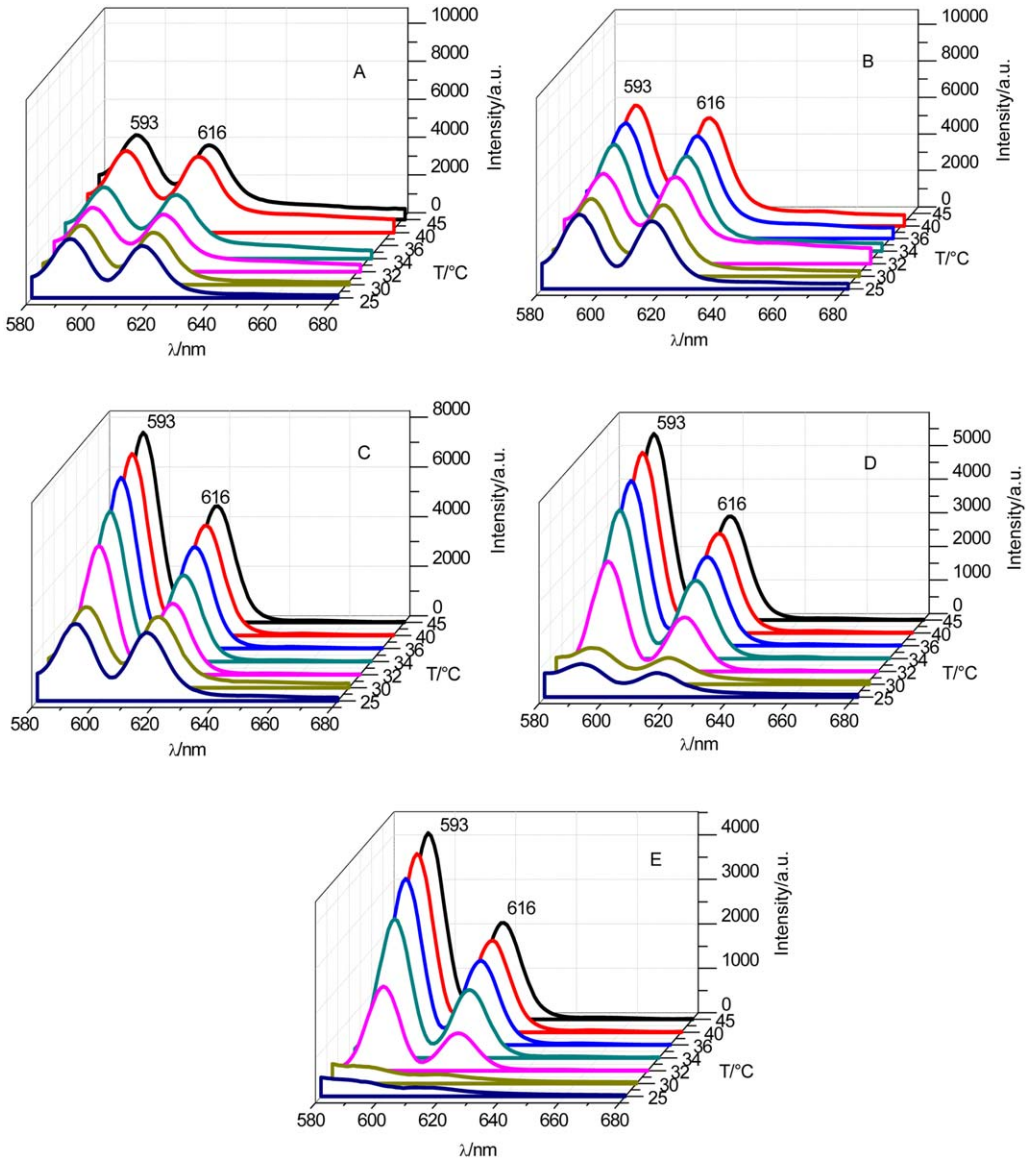

Figure 5. The PL spectra of the core–shell nanogels at varied ambient temperature with different content in water: (A) 10 wt %, (B) 20 wt %, (C) 40 wt %, (D) 60 wt %, and (E) 80 wt %. [Color figure can be viewed in the online issue, which is available at wileyonlinelibrary.com.]

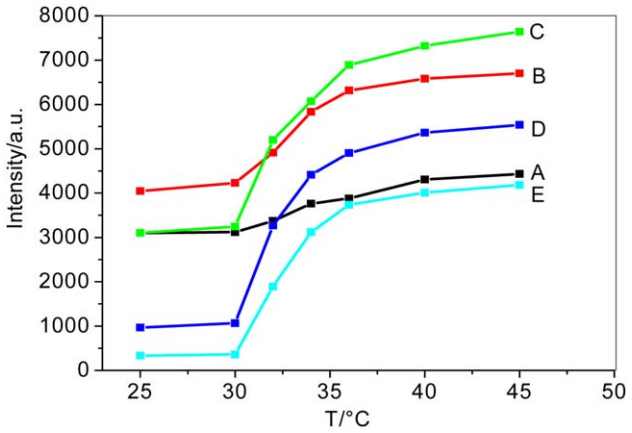

Figure 6. PL intensity of the nanogels at 593 nm as a function of temperature: (A) 10 wt %, (B) 20 wt %, (C)40 wt %, (D) 60 wt %, and (E) 80 wt %. [Color figure can be viewed in the online issue, which is available at wileyonlinelibrary.com.]

nanogels become weak again, but their temperature induced PL transition is still very drastically. The inclination of fluorescence intensity of the nanogels at high concentration may be resulted from the concentration quenching of the nanogels.

Drug Release Behavior of the Nanogels

Nowadays, drug loading and releasing behavior is an interesting area for nanogels. In order to reveal the drug loading and release behavior and the related mechanism, Aspirin was used as a model drug to assess the loading and controlled releasing behavior of the core–shell nanogels. The PL spectra of the nanogels with varied concentration of Aspirin ($\lambda_{ex} = 300$ nm) was recorded in Figure 7, and the PL intensity of the nanogels at 593 nm with different content of Aspirin is plotted in Figure 7(C). As the results shown in Figure 7(C), with increasing the concentration of Aspirin, the intensity of the nanogels became weak correspondingly.

To explain the mechanism of Aspirin quenches the emission of the PL nanogels, UV–vis spectrum of Aspirin was carried out. As the spectrum shown in Figure 7(D), the absorbing range of Aspirin is in 280–320 nm, and the most intensive absorbing peak is centered on 297 nm. Due to the wavelength of the exciting wave is 300 nm, implying that, when Aspirin and the nanogels co-exist in a mixed system, the exciting wave of the nanogels will be absorbed by the loaded Aspirin. Hence, only part of the energy from the exciting wave can be transferred to the nanogels to emitting PL. And the higher the concentration of the loaded Aspirin, the weaker the fluorescence intensity of the nanogels is recorded.

In order to investigate the drug release behavior for the nanogels, the drug release curves of the nanogels were obtained by PL test. As the spectra recorded in Figure 8, with the prolongation of time, the intensity of the nanogels became intensive gradually. As the curves shown in Figure 8(C), with the prolongation of time, the release rate of Aspirin increased gradually, but the drug release behavior was affected greatly by the

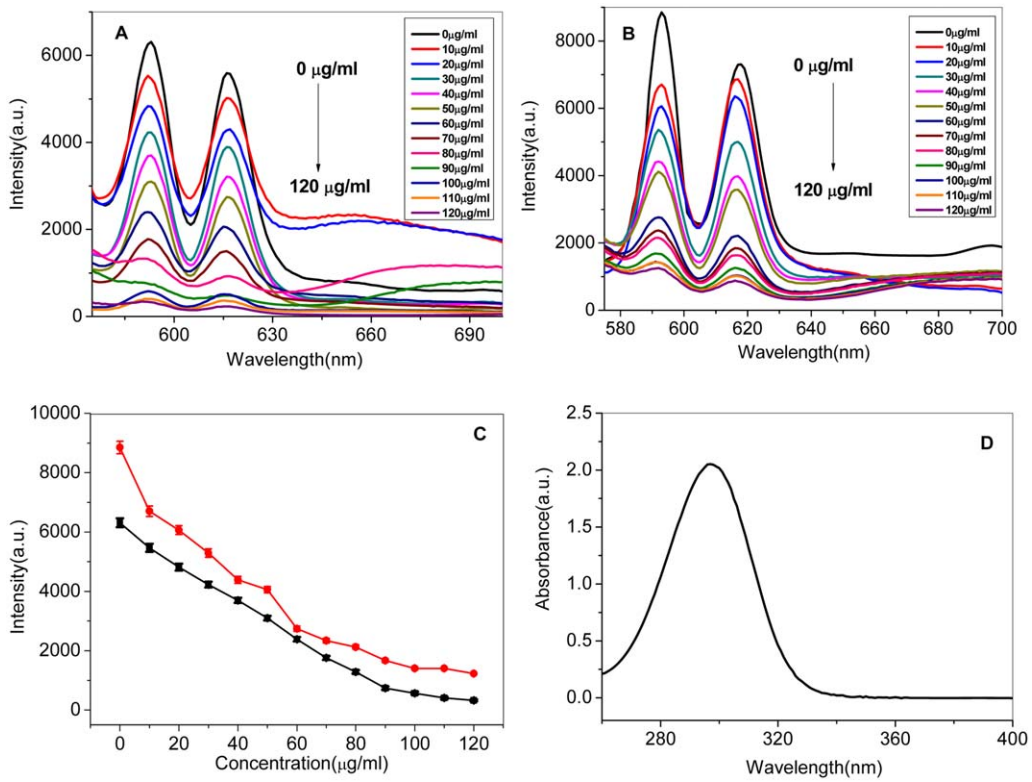

Figure 7. The PL spectra of the nanogels with varied concentration of Aspirin ($\lambda_{ex} = 300$ nm): (A) 25°C and (B) 37°C. (C) The PL intensity of the nanogels at 593 nm with different content of Aspirin. (D) The UV–vis spectrum of Aspirin (H_2O solution, room temperature, C = 50 μg/mL). [Color figure can be viewed in the online issue, which is available at wileyonlinelibrary.com.]

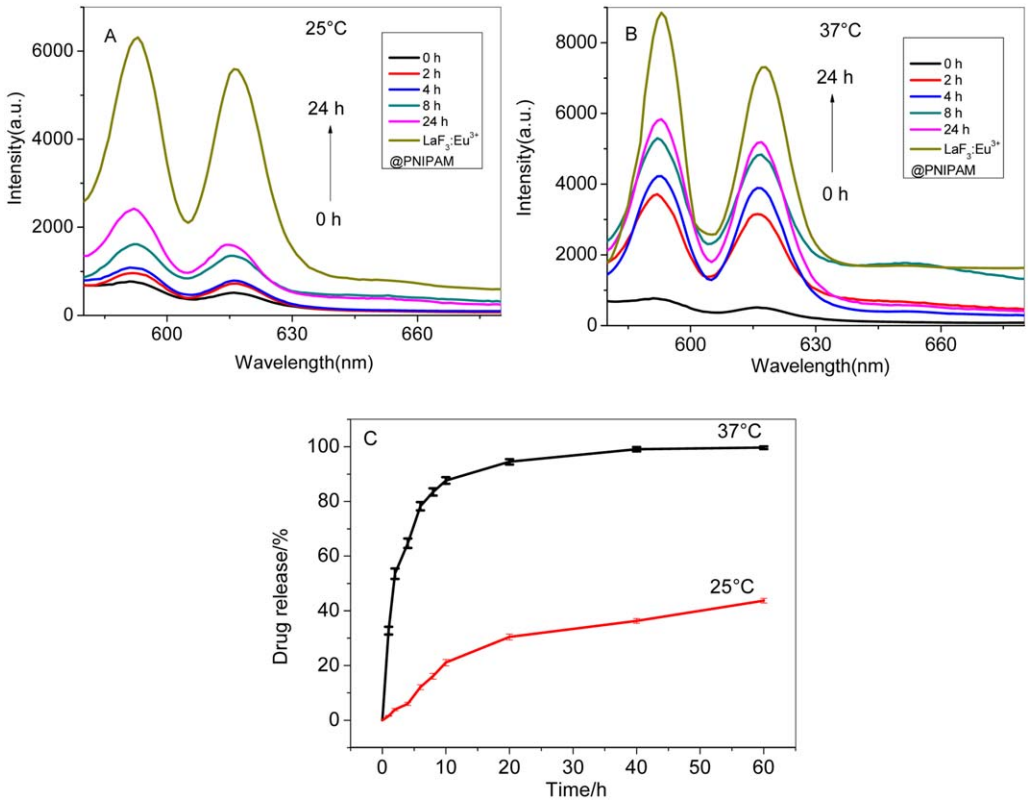

Figure 8. The PL spectra of the Aspirin loaded nanogels at different time ($\lambda_{ex} = 300$nm): (A) 25°C and (B) 37°C. (C) The drug release curves of the nanogels. [Color figure can be viewed in the online issue, which is available at wileyonlinelibrary.com.]

ambient temperature. For instance, when the test was kept at 25°C (<LCST), only 43.7% of the total amount of the absorbed Aspirin was released in 60 h; and the release rate of Aspirin was very low. While the test was carried at 37°C, a temperature similar to human body (>LCST), a similar release rate of Aspirin (~43%) had been reached in only about 2 h, and about 99.7% of the total amount of the absorbed Aspirin had been released in 60 h.

This unique drug release phenomena may be resulted from the thermo-induced phase transition of the nanogels. At the temperature of 37°C, that was higher than the nanogels LCST, the shell of PNIPAM shrunk greatly, and large parts of water was repelled from the nanogels. Due to Aspirin is a water soluble compound, it may be released with the repelled water.

CONCLUSIONS

Novel core–shell nanogels of LaF_3 : Eu^{3+} nanocrystals/PNIPAM have been synthesized via surface initiated ATRP strategy, and their thermosensitive fluorescence performance and drug release behavior, as well as the mechanism, were investigated in details. The results suggested that the fluorescence performance of the nanogels is affected greatly by ambient temperature and relative content of which in water. Due to the interaction of the nanogels and Aspirin, the PL intensity of the nanogels varied considerably with variation of drug concentration, this unique performance made the drug release behavior of nanogels to be traceable.

REFERENCES

1. Mimi, H.; Ho, K. M.; iu, Y. S.; Wu, A.; Li, P. *J. Controlled Release* **2012**, *148*, 123.
2. Richtering, W.; Pich, A. *Soft Matter* **2012**, *8*, 11423.
3. Zhang, J.; Chu,L. Y.; Cheng, C. J.; Mi, D. F.; Zhou, M. Y.; Ju, X. J. *Polymer* **2008**, *49*, 2595.
4. Stuart,M. A. C.; Huck, W. T. S.; Genzer, J.; Mueller, M.; Ober, C.; Stamm, M.; Sukhorukov, G. B.; Szleifer, I.; Tsukruk, V. V.; Urban, M.; Winnik, F.; Zauscher, S.; Luzinov, I.; Minko, S. *Nat. Mater.* **2010**, *9*, 101.
5. Zhang, J. T.; Jandt, K. D. *Macromol. Rapid Commun.* **2008**, *29*, 593.
6. Zhang, J. T.; Liu, X. L.; Fahr, A.; Jandt, K. D. *Colloid. Polym. Sci.* **2008**, *286*, 1209.
7. Burmistrova, A.; Von Klitzing, R. *J. Mater. Chem.* **2010**, *20*, 3502.
8. Zhu, Y.; Kaskel, S.; Ikoma, T.; Hanagata,N. *Microporous Mesoporous Mater.* **2009**, *123*, 107.
9. Duan, C. X.; Zhang, D. R.; Wang, F. H.; Zheng, D. D.; Jia, L. J.; Feng, F. F.; Liu, Y.; Wang, Y. C.; Tian, K. L.; Wang, F. S.; Zhang, Q. *Int. J. Pharm.* **2011**, *409*, 252.
10. Li, W.; Guo, Q.; Zhao, H.; Zhang, L.; Li, J.; Gao, J.; Qian, W. Z.; Li, B. H.; Chen, H. W.; Wang, H.; Dai, J. X.; Guo, Y. J. *Nanomedicine* **2012**, *7*, 383.
11. Yallapu, M. M.; Vasir, J. K.; Jain, T. K.; Vijayaraghavalu, S.; Labhasetwar, V.; Biomed, J. *Nanotechnol.* **2008**, *4*, 16.

12. Scherzinger, C.; Lindner, P.; Keerl, M.; Richtering, W. *Macromolecules* **2010**, *43*, 6829.
13. Huang, G.; Hu, Z. *Macromolecules* **2007**, *40*, 3749.
14. Pagariya, T. P.; Patil, S. B. *Colloids Surf., B* **2013**, *102*, 171.
15. Nasir, F.; Iqbal, Z.; Khan, J. A.; Khan, A.; Khuda, F.; Ahmad, L. *Int. J. Pharm.* **2012**, *439*, 120.
16. Karthikeyan, K.; Guhathakarta, S.; Rajaram, R.; Korrapati, P. S. *Int. J. Pharm.* **2012**, *438*, 117.
17. Nippe, S.; General, S. *Eur. J. Pharm. Sci.* **2012**, *47*, 790.
18. Grzyb, T.; Lis, S. *J. Rare Earth* **2009**, *27*, 588.
19. Wang, Z.; Li, M.; Wang, C.; Chang, J.; Shi, H.; Lin, J. *J. Rare Earth* **2009**, *27*, 33.
20. Sudarsan, V.; Sivakumar, S.; Veggel, F.; Raudsepp, M. *Chem. Mater* **2005**, *17*, 4736.
21. Li, C.; Zhang, C.; Hou, Z.; Wang, L.; Quan, Z.; Lian, H. *J. Phys. Chem. C* **2009**, *113*, 2332.
22. Chen, D.; Yu, Y.; Huang, P.; Lin, H.; Shan, Z.; Wang, Y. *Acta Mater.* **2010**, *58*, 3035.
23. Dai, Y. L.; Ma, P. A.; Cheng, Z. Y.; Kang, X. J.; Zhang, X.; Hou, Z. Y.; Li, C. X.; Yang, D. M.; Zhai, X. F.; Lin, J. *ACS Nano* **2012**, *6*, 3327.
24. Song, Q. S.; Yang, Y.; Gao, K.; Ma, H. H. *J. Lumin.* **2013**, *136*, 437.
25. Song, Q. S.; Yang, Y.; Zhu, X. F. *Chem. J. Chinese U.* **2012**, *33*, 1084.
26. Song, Q. S.; Zhu, X. F.; Yang, Y. *Acta Polym. Sin.* **2012**, *4*, 442.
27. Song, Q. S.; Gao, K.; Yao, W.; Yang, Y.; Ma, H. H. *Acta Chim. Sinica* **2012**, *70*, 2155.
28. Meng, J. X.; Zhang, M. F.; Liu, Y. L.; Man, S. Q. *Spectrochim. Acta, Part A* **2007**, *66*, 81.